A&A 406, L5–L8 (2003)
DOI: 10.1051/0004-6361:20030818

Astronomy & Astrophysics

Letter to the Editor

Solar active regions: The footpoints of 1 MK loops

G. Del Zanna⋆

Department of Applied Mathematics and Theoretical Physics, University of Cambridge, UK

Received 26 March 2003 / Accepted 31 May 2003

Abstract. On-disc SOHO and TRACE observations of the footpoints of 1 MK quiescent loops in a solar active region are presented. These types of loops are long-lived and high-lying features that are best seen in the TRACE 173 Å passband, sensitive to 1 MK temperatures. SOHO/CDS data are used to show the clear association between the high-lying 1 MK coronal emission and emission formed at lower heights and temperatures, in the transition region. The 1 MK loops are rooted in strong unipolar regions located at the supergranular network boundaries. These loops have near-isothermal distributions at each location along their length, with peak emission measures at $T = 0.7$ MK, where electron densities are $\sim 2 \times 10^9$ cm^{-3}. The loops showed photospheric abundances, at odds with previous results based on Skylab data.

Key words. Sun: corona – Sun: transition region – Sun: abundances – techniques: spectroscopic

1. Introduction

One of the common features in the Transition Region and Coronal Explorer (TRACE) and SOHO/EIT (EUV Imaging Telescope) images of active regions (ARs) in the EUV passbands centred around 173 Å are high-lying and long-lived loops having temperatures $T \simeq 10^6$ K (see the review by Schrijver et al. 1999). The properties of these "1 MK loops" are presented in detail by Del Zanna & Mason (2003) using off-limb TRACE and SOHO/CDS (Coronal Diagnostic Spectrometer) observations. Most of their results are at odds with the current literature. The loops were found to have decreasing temperatures toward their bases and to be nearly isothermal at each location along their length. One drawback with that analysis was that the loop footpoints were not clearly visible.

The aim of this paper is to use on-disc SOHO and TRACE observations to describe the general properties of the 1 MK loop footpoints in terms of densities, temperatures, elemental abundances, and their relation to the underlying photospheric magnetic field. The literature of on-disc AR observations is extensive, but there are virtually no detailed studies where the footpoints of these 1 MK loops are clearly identified. It turns out that these footpoints produce strong emission in transition region (TR) lines formed in the range $T = 0.1–0.8$ MK. The TRACE bandpasses do not provide sufficient information in this temperature range. The CDS observes emission lines formed over a large temperature range, from chromospheric to coronal temperatures, and is therefore the ideal instrument to complement the TRACE observations.

Before SOHO, many AR studies were based on the Skylab SO82A slitless spectrometer. This instrument produced overlapping spectroheliograms that could only provide partial information for bright compact sources. For this reason, many studies (e.g. Widing & Feldman 1993; Sheely 1996; Widing 1997; Widing & Feldman 2001) were limited to analyses of the footpoints of AR loops, some of which might have been associated with the same type of 1 MK quiescent loops that are discussed here. In particular, most studies focused on measurements of Ne/Mg relative abundances. Elemental abundances were found to differ from photospheric values in a way related to the first ionization potential (FIP) of these elements (see e.g. Raymond et al. 2001). The main well-established results from Skylab data were: 1) newly born active regions show a "photospheric" Mg/Ne relative abundance ($A_{\rm Mg/Ne} = 0.32$, FIP bias = 1); 2) the FIP bias increases in a matter of hours, reaching coronal values ($A_{\rm Mg/Ne} = 1.4$, FIP bias = 4) just after a day or two, and values up to 7–9 in 3–7 days. Detailed studies of FIP bias variations are of great importance in stellar physics since they can give us clues to an understanding of the (still unknown) basic physical processes at work in the element fractionation.

SOHO/CDS observations have been used by Young & Mason (1997) and Fletcher et al. (2001) to study active region brightenings. Transition region densities $N_{\rm e} \simeq 10^9$ cm^{-3} were found. The observed brightenings showed a strong variability in their Mg/Ne relative abundances, with FIP biases in the range 1 to 9. However, as in the case of the Skylab results, the relationship between the brightenings, the underlying photospheric field and the overlying coronal structures was not clearly defined.

2. Observations and results

On 1998 May 13 TRACE (with all its filters) and CDS (with the Normal Incidence Spectrometer-NIS) simultaneously

⋆ e-mail: G.Del-Zanna@damtp.cam.ac.uk

observed NOAA 8219 for most of the day, close to meridian. The main features of this quiescent active region remained the same throughout the day. NOAA 8219 was an ordinary small bipolar AR with a minute sunspot, no filaments and no significant flaring activity. It was already well developed on May 7 when it was close to the east limb. The dataset analysed is vast and includes Yohkoh/SXT, SOHO/MDI, EIT, CDS and ground-based observations over a time span of many days. Here, only CDS observations on May 13, complemented by TRACE and SOHO/MDI near-simultaneous data, are presented. The instruments, data analysis and diagnostic methods used here are the same as those used and described in detail in Del Zanna & Mason (2003). Here we note that the CDS study AR_MON contained a large number of lines emitted from chromospheric to coronal temperatures. The CDS field of view (FOV $= 4 \times 4'$) was covered by scanning the $4 \times 240''$ slit from West to East between 07:50 and 08:46 UT. The CDS calibration by Del Zanna et al. (2001a) and the CHIANTI package (v. 4.02, Young et al. 2003) have been used. The pixel resolutions of the MDI, TRACE and CDS data presented here are $2 \times 2''$, $0.5 \times 0.5''$and $4 \times 3.36''$ along the E-W and N-S directions ($1'' \simeq 730$ km). The various observations have been accurately co-aligned. *DEM* analyses were performed, but here only results from the emission measure (EM) loci method are presented. The method (see Del Zanna et al. 2002 for details) is to plot the ratio between the observed intensities and the contribution functions as a function of T, to constrain the EM values and to estimate the elemental abundances. This method is particularly useful when the emission is nearly isothermal because in this case all the curves should cross at one point.

AR 8219 had many 1 MK loops. Only the loop legs are clearly visible in the TRACE 173 Å images. Figure 1 shows the first loop leg, that has a typical comet-shaped morphology as observed in the TRACE 173 Å bandpass. This loop leg was approximately aligned along the N-S direction and had the corresponding footpoint (of the opposite polarity) outside the TRACE FOV. The TRACE 173 Å image has a correspondence in the CDS lines formed at $T = 1$ MK (e.g. Mg IX), as expected, since the TRACE 173 Å passband mainly observes Fe IX and Fe X, which are formed at 1 MK. On the other hand the TRACE 195 Å image, commonly thought to be dominated by Fe XII emission, does not have a correspondence with the CDS Fe XII image, where no emission is present. The TRACE 195 Å band is most probably dominated by lower-temperature Fe VIII lines, which make diagnostics based on this band unreliable. These issues are discussed in detail in Del Zanna & Mason (2003). Figure 1 shows that the maximum emission in Mg IX is located in region A3, while the peak emission in lines that are formed at progressively lower temperatures shifts southward. The peak emission in TR lines (Mg VII, $T = 0.6$ MK) is located in region A2, while the footpoint is located in region A1, clearly visible as a compact emission in the lower transition region lines such as O III, Ne V (see O V, $T = 0.25$ MK). The region A1 corresponds to a strong photospheric unipolar region.

The fact that the loop leg is only visible in lines formed in a restricted temperature range, having peak emission located at different spatial positions, is an obvious consequence

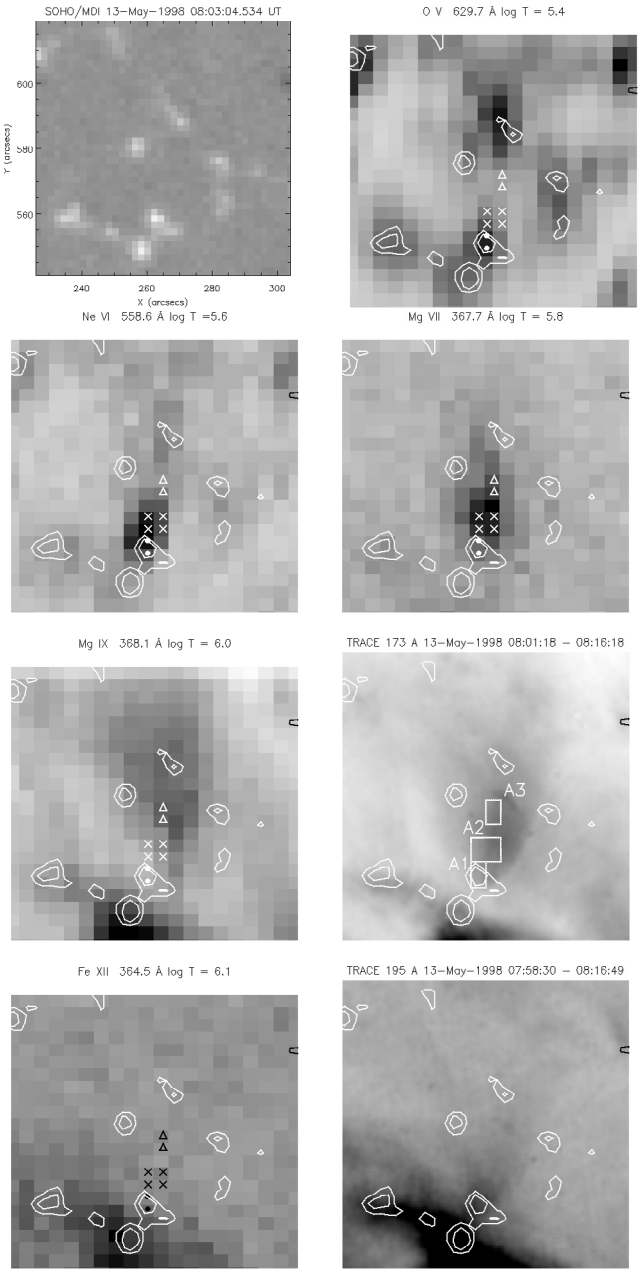

Fig. 1. MDI magnetogram, CDS monochromatic and TRACE negative images of a 1 MK loop. MDI magnetogram isocontours (50, 100 G) are displayed on the CDS and TRACE images. Regions A1, A2, A3, corresponding to the loop visibility at $T \simeq 0.1$–0.3 (O V), 0.6 (Mg VII) and 1 MK (Mg IX) are displayed on the CDS images with different symbols and with their contours on the TRACE 173 Å image.

of its thermal structure. This characteristic, together with the fact that the observed lines are optically thin, has a few important consequences from a diagnostic point of view. First of all, the loop is almost isothermal at each location along its length. This is confirmed by EM analyses. An example is provided in Fig. 2, where the EM curves of region A2, crossing approximately at $\log T = 5.85$, are displayed. Second, the loop leg has a steep temperature gradient in just a few CDS pixels. This, together with the fact that the tilt of the

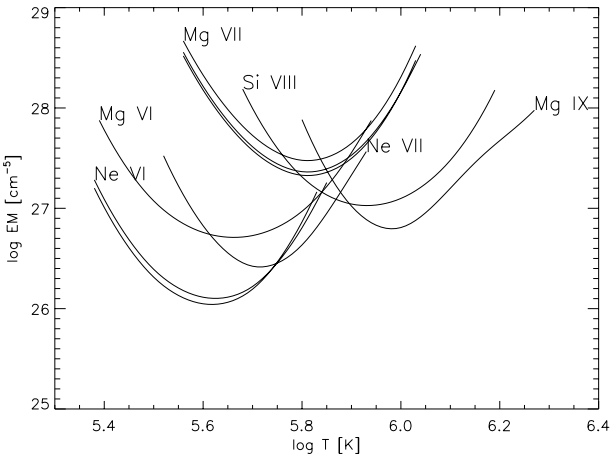

Fig. 2. Emission measure curves for region A2. The curves were calculated with: the ionization tables of Mazzotta et al. (1998); the photospheric abundances of Grevesse & Sauval (1998) with the oxygen abundance corrected to a value of 8.7 (N. Grevesse 2000, priv. comm.); and $N_e = 2 \times 10^9$ cm^{-3}.

loop is unknown, makes accurate measurements of temperatures and densities along its length difficult. However, accurate measurements at $T = 0.6$ MK can be obtained with the use of the Mg VII 319.0/367.7 Å density-sensitive ratio as shown in Table 1. Third, only results that use lines formed in a limited temperature (hence height) range can be valid. In particular, this is important when studying elemental abundances. For example, the relative O/Ne abundance is well constrained at $T = 0.2$ MK by O V and Ne V lines that are only observed in region A1. Transition region lines such as Ne VI, Ne VII, Mg VI, Mg VII, Si VIII, Ca X are only observed in a limited spatial area (region A2). Abundance measurements involving Ne, Mg, Si, and Ca can only be provided for that area. The results for this loop are consistent with photospheric abundances. Fourth, line-of-sight contamination of background and foreground emission makes all measurements of loop characteristics subject to some additional uncertainty. Del Zanna & Mason (2003) have shown that this contamination has a major effect on the results derived from off-limb observations because of the long path lengths. In the on-disc case, contamination is generally smaller. Averaged background intensities have been obtained from a nearby quiet Sun cell-centre region and subtracted from the loop line intensities before any subsequent analysis (EM, density). The TR lines used here are very bright at the loop base locations and contamination is small (of the order of 10%).

Two other 1 MK loop bases were analysed in detail. One is shown in Fig. 3. As in the case of the first loop, a few regions were selected for further analysis. Table 1 presents the electron densities of the various areas at the Mg VII heights. All the loops analysed presented the same characteristics as the first loop. In particular, in terms of abundances all the loops had photospheric abundances (although uncertainties related to the ion fractions are large – say a factor of 2). This is at odds with the Skylab results since this active region emerged at least 5 days before and should have a large FIP bias. It could well be that not all active regions present a FIP-bias trend or that the

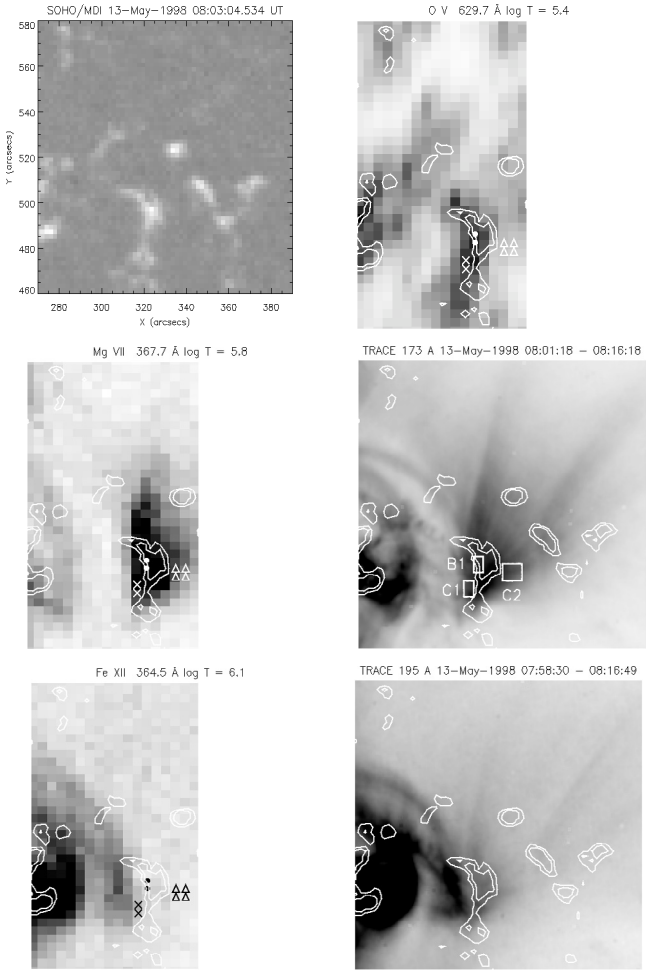

Fig. 3. As Fig. 1, for the fan of 1 MK loops.

Table 1. Electron densities N_e derived from the Mg VII 319.0/367.7 Å ratio R for the regions shown in Figs. 1, 3.

Region	R (counts)	R (erg)	N_e (10^9 cm^{-3})
A2	0.19 ± 0.03	0.54 ± 0.08	1.9 ± 0.7
A3	0.10 ± 0.04	0.28 ± 0.10	0.6 ± 0.3
B1	0.19 ± 0.01	0.55 ± 0.04	1.9 ± 0.4
C1	0.22 ± 0.03	0.63 ± 0.09	2.6 ± 1.0
C2	0.18 ± 0.01	0.52 ± 0.04	1.7 ± 0.3

AR loops observed with Skylab SO82A were different types of loops. A more probable explanation is that a FIP bias of a loop is related to the lifetime of the magnetic fragments at its footpoints and not to the age of the active region.

Another possibility is that the results based on Skylab overestimated the FIP bias. Del Zanna et al. (2001b) and Del Zanna et al. (2003) have already shown that previous results based on Skylab data seriously overestimated the FIP bias (up to a factor of 10 for coronal hole plumes). This was mainly caused by the use of approximate diagnostic methods. To test this possibility, the Widing & Feldman (1993) active region data have been re-analysed, with the use of more recent atomic calculations. Widing & Feldman (1993) measured TR line intensities

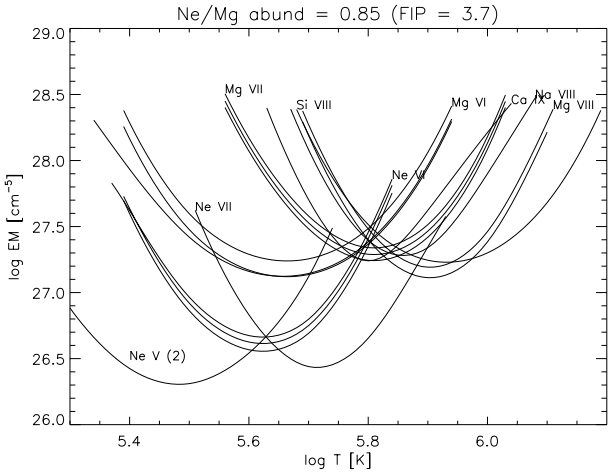

Fig. 4. *EM* curves of the Skylab data of Widing & Feldman (1993) calculated with the coronal abundances of Feldman (1992) and the ionization tables of Mazzotta et al. (1998).

at the footpoint of an AR loop and found a large FIP bias of 14 ($A_{\rm Mg/Ne} = 4.4$ assuming a photospheric $A_{\rm Mg/Ne} = 0.32$). The line intensities provided by Widing & Feldman (1993) have been used to compute the *EM* curves, which are shown in Fig. 4. Quite surprisingly, the data are consistent with a FIP bias of only 3.7 ($A_{\rm Mg/Ne} = 1.18$). This suggests that previous results based on Skylab data overestimated the FIP bias by large factors also for active regions. The remarkable similarities between the *EM* curves of Fig. 4 and those of Fig. 2 suggest that the footpoint studied by Widing & Feldman (1993) could have been associated with the same 1 MK loops discussed here.

3. Summary and conclusions

On-disc SOHO and TRACE observations of the footpoints of 1 MK quiescent loops show a clear relation between the emission in the corona ($T \simeq 1$ MK), the transition region ($T = 0.2$–0.9 MK) and the photosphere. The loops are rooted in strong unipolar regions that are located at or near the supergranular network boundaries. These loops have near-isothermal distributions at each location along their length. Their temperature has a steep increase in the transition region around $T = 0.7$ MK, where emission measures peak and electron densities are $\simeq 2 \times 10^9$ cm^{-3}. These results confirm and extend those of Del Zanna & Mason (2003), where off-limb observations were presented and discussed in more detail. Various effects that complicate the analysis and the interpretation of observations of active region loops have been discussed. TRACE data have severe limitations in their diagnostics, while CDS data are excellent for temperature and for some elemental abundance diagnostics. To accurately determine densities, spectroscopic instruments that measure density-sensitive ratios of lines that are formed at the various loop temperatures would be needed. This is something that future instruments should address.

The observed 1 MK loops did not show a FIP effect, which is at odds with previously well-established results based on Skylab data. The fact that Widing & Feldman (1993) probably overestimated the FIP bias by a factor of 4 suggests that the results based on Skylab data need revision. However, it should be kept in mind that previous results on active region FIP bias variations might apply to different types of loops.

Despite decades of studies the general properties of the 1 MK quiescent loops are described for the first time in some detail here and in Del Zanna & Mason (2003). Previous studies of AR loops either do not apply to this class of loops or contain results that need to be revised. More work on both the observational and theoretical side is still needed to characterise these 1 MK loops, that are among the most common features in solar active regions.

Acknowledgements. Support from PPARC is acknowledged. I wish to thank the anonymous referee for detailed comments that helped to improve the manuscript. SOHO is a project of international collaboration between ESA and NASA. TRACE is a NASA Small Explorer (SMEX) mission.

References

Del Zanna, G., Bromage, B. J. I., Landi, E., & Landini, M. 2001a, A&A, 379, 708
Del Zanna, G., Bromage, B. J. I., & Mason, H. E. 2001b, AIP Conf. Proc., 598, 59
Del Zanna, G., Bromage, B. J. I., & Mason, H. E. 2003, A&A, 398, 743
Del Zanna, G., Landini, M., & Mason, H. E. 2002, A&A, 385, 968
Del Zanna, G., & Mason, H. E. 2003, A&A, in press
Feldman, U. 1992, Phys. Scr, 46, 202
Fletcher, L., López Fuentes, M. C., Mandrini, C. H., et al. 2001, Sol. Phys., 203, 255
Grevesse, N., & Sauval, A. J. 1998, Space Sci. Rev., 85, 161
Mazzotta, P., Mazzitelli, G., Colafrancesco, S., & Vittorio, N. 1998, A&AS, 133, 403
Raymond, J. C., Mazur, J. E., Allegrini, F., et al. 2001, AIP Conf. Proc., 598, 49
Schrijver, C. J., Title, A. M., Berger, T. E., et al. 1999, Sol. Phys., 187, 261
Sheeley, N. R. 1996, ApJ, 469, 423
Widing, K. G. 1997, ApJ, 480, 400
Widing, K. G., & Feldman, U. 1993, ApJ, 416, 392
Widing, K. G., & Feldman, U. 2001, ApJ, 555, 426
Young, P. R., Del Zanna, G., Landi, E., et al. 2003, ApJS, 144, 135
Young, P. R., & Mason, H. E. 1997, Sol. Phys., 175, 523